Structure and magnetism of ultrathin epitaxial Fe on Ag(100)

A. Hahlin,[1] C. Andersson,[1] J. Hunter Dunn,[2] B. Sanyal,[3] O. Karis,[1] and D. Arvanitis[1]
[1]*Department of Physics, Uppsala University, Box 530, SE-751 21 Uppsala, Sweden*
[2]*Max-Laboratory, Lund University, Box 118, SE-221 00 Lund, Sweden*
[3]*Theoretical Magnetism Group, Uppsala University, Box 530, SE-751 21 Uppsala, Sweden*
(Received 10 March 2005; revised manuscript received 16 November 2005; published 26 April 2006)

We have made *in-situ* investigations of ultrathin films of Fe grown on a Ag(100) single crystal. This system is known to exhibit a reorientation of the magnetization, dependent on both Fe thickness and temperature. X-ray absorption fine structure has been recorded for samples prepared *in-situ*, both in the near edge and in the extended x-ray absorption fine structure (EXAFS) region. Using x-ray magnetic circular dichroism we found that Fe films between 2–5 monolayers show an out-of-plane remanent magnetization. For thicker films the magnetization lies in-plane. By applying the magneto-optical sum rules we found an enhancement of the orbital moment (m_l) for the out-of-plane phase, whereas the spin moment (m_s) is unchanged. From the Fe *L*-edge EXAFS, we obtain information on the local crystallographic structure. A strong correlation between the local crystallographic structure and the magnetic properties is found for the Fe/Ag(100) system. Variations in the nearest neighbor distance of ~0.15 Å are observed when comparing 3 ML and 25 ML films. By comparison to simulations performed with the FEFF 8.10 code, we can identify a bcc structure for 6–25 ML Fe on Ag(100). For the 3 ML Fe film our simulations indicate strong deviations from any structure derived along the Bain path. We conclude that intermixing and distortion are important to describe the structure in this thickness range.

DOI: 10.1103/PhysRevB.73.134423 PACS number(s): 75.70.−i, 61.10.Ht, 79.60.Dp, 78.70.Dm

I. INTRODUCTION

The magnetic anisotropy in ultrathin films is often very different to that found in the bulk. This phenomenon has been widely studied both experimentally and theoretically, but the fundamental role of the interfaces in modifying the magnetization of these films is still unclear. Of particular interest is the spin reorientation transition (SRT), which has been shown to be dependent on film thickness, temperature, and also cap layer thickness.[1] The epitaxial growth of transition metal ultrathin films on surfaces of noble metals provides excellent opportunities for the investigation of low dimensional magnetism. Here we present x-ray magnetic circular dichroism (XMCD) and extended x-ray absorption fine structure (EXAFS) investigations of Fe films deposited onto a Ag(100) single crystal substrate. Theoretical investigations of Fe on Ag(100) indicate a strong correlation between real space structure and the Fe magnetic moment.[2,3] In the present investigation we correlate the magnetic properties to the local crystallographic structure of the Fe/Ag(100) system.

The Fe/Ag(100) system is known to undergo a SRT from in-plane to out-of-plane magnetization as the Fe thickness or the sample temperature is lowered.[4,5] Below 300 K this SRT occurs at a Fe thickness of ~6 ML.[5] Here the surface anisotropy, favoring an out-of-plane easy axis, overcomes contributions that favor an in-plane easy axis. These contributions include the magnetocrystalline anisotropy of the interior of the film and the demagnetizing field. The out-of-plane magnetization for a free standing Fe layer was predicted by Gay *et al.*[6] and later confirmed experimentally.[7,8]

Besides the SRT, the size of the Fe magnetic moment is thickness dependent. Using SQUID magnetometry, Wooten *et al.*[9] reported an enhancement of the magnetic moment of 25% above the bulk Fe moment as the film thickness was decreased. Theoretical investigations verify both the enhanced magnetic moment as the film thickness is decreased[2,3,10–12] and the SRT thickness.[3] Recently, Lazarovits *et al.*,[13] addressing lower dimensions, reported even higher magnetic moments for Fe clusters deposited on Ag(100).

Using the magneto-optical Kerr effect, Berger *et al.*[14] reported a decay of the remanent out-of-plane magnetization over time. This effect was found to be important for temperatures above 120 K. The authors also report a strong decay of the remanent out-of-plane magnetization for a 4.3 ML Fe film at 120 K. However, these films were heat treated to 440 K which not only improves the LEED pattern but also introduces increased intermixing between the Fe film and the Ag substrate. Canepa *et al.*[15] have studied the growth of the Fe/Ag(100) system in detail and highlight a number of parameters that influence the epitaxy, e.g., substrate quality, deposition rate and temperature and annealing procedures. In particular, they discuss the importance of the intermixing between the film and substrate occurring predominantly above 200 K.

The influence of the above-mentioned parameters might be the reason for the apparently contradictory results reported in early works on the Fe/Ag(100) system. Initially, Li *et al.*[16] reported that bcc Fe can be stabilized on Ag(100). The same group also claimed that their LEED investigations showed neither a Frank-van der Merwe (layer-by-layer) nor a Stranski-Krastanov [layer-by-layer accompanied with a three-dimensional (3D) island growth] growth mode.[10] This is in contrast to a reflection high energy electron diffraction study[17] which indicated a layer-by-layer growth up to at least

nine Fe layers for samples grown at low temperature (77 K) and five to six layers at room temperature. Moreover, Ciccacci *et al.*[18] reported a poor crystalline quality of the film with increasing disorder when going from Au to Cu to Ag as substrates. More recently, Canepa *et al.*[15] found that between 2 and 5 ML the Fe film morphology gradually deviates from the two-dimensional (2D) growth towards island growth.

Until now, no attempts to separately determining the orbital (m_l) and spin (m_s) magnetic moments have been reported. Recently we presented an XMCD and EXAFS investigation characterizing the SRT and suggested further investigations concerning the local crystallographic structure.[19] Here we present data obtained for three different Fe films on Ag(100), namely the out-of-plane phase (3 ML); the phase in the vicinity of the SRT (6 and 8 ML); and the in-plane phase (25 ML). From the XMCD data we determine the m_l and m_s in μ_B per atom.[20,21] Under identical experimental conditions, i.e., within the same sample preparation, we combine our *in situ* XMCD measurements with *in situ* *L*-edge EXAFS measurements in order to provide information on the local crystallographic structure. *L*-edge EXAFS experiments on thicker Fe films have been reported earlier by Lemke *et al.*,[22] for the Fe/Cu(100) system. In this work, Fe was reported to adopt the bulk like bcc structure. Jaffres *et al.*[23] preformed a *K*-edge EXAFS investigation on a 50 Å Fe film deposited on a MgO substrate. The Fe crystallographic structure was shown to be body-centered tetragonal with an expansion in the film plane and a compression in the perpendicular direction as compared to the bulk bcc. For 3*d* transition metals, *K*-edge EXAFS offers some distinct advantages above *L*-edge EXAFS, but in our case the possibility of using both XMCD and *L*-edge EXAFS within the same film preparation is valuable and worthwhile.

II. EXPERIMENT

The XMCD and EXAFS results were obtained at beamline D1011 of MAX-lab. This bending-magnet beamline is comprised of a modified SX700 monochromator that covers the energy range 30 to 1500 eV. The fairly smooth distribution of intensity over the whole energy interval makes it suitable for *L*-edge EXAFS of 3*d* transition metals. The beamline offers the elliptically polarized x rays necessary for the XMCD measurements. The degree of circular polarization of the x rays (p_c) has been measured to be of order 0.85.[24] The XMCD contrast was obtained by reversing the magnetization of the sample using a dc field of 0.6 kOe, the helicity of the light remaining fixed. All measurements were done in remanence, i.e., without applying a field during data acquisition. The photon energy resolution was set to 0.8 eV and 1.5–3 eV for the XMCD and EXAFS measurements, respectively. The beam spot size at the sample is 1 mm vertical and horizontal.

In addition to the EXAFS measurements we performed EXAFS simulations using the FEFF 8.1 code. Simulations were made for "bulklike" bcc, bct, and fcc Fe. We also simulated Fe/Ag layered systems, with 3 Fe ML on top of 6 ML Ag(100), and for models where intermixing at the interfaces was taken into account. Scattering events occurring within an 8 Å radius of the absorbing atom were considered. In the modeling the temperature was set to 120 K and the Debye temperature to 477 K (as for Fe bulk).

The Ag(100) single crystal substrate surface was cleaned by argon ion bombardment followed by annealing until sharp LEED patterns were observed, indicating a well-defined long range order. Typical parameters for these cycles were sputtering for 20 minutes at 2.0 keV and 5 μA, followed by annealing the crystal at 900 K for 2 minutes. For the last cycle we used a lower voltage and at a shorter time; 5 minutes sputtering below 1.0 keV and 2 μA. The cleanliness of the substrate was checked by means of x-ray photoelectron spectroscopy (XPS). For the C1*s* and O1*s* spectra an excitation energy of 700 eV was used. As a rule of thumb this implies that the level of C or O contaminants was below 0.01 ML. For several of the samples XPS measurements were also performed for the Fe overlayers to investigate the cleanliness. In all investigated cases we estimate the level of C and O contamination to be below 0.05 ML, meaning that no or barely detectable signals from contaminants were observed in the C1*s* and O1*s* spectra.

The films were grown following the recipe of Canepa *et al.*[15] that includes two steps: deposition at low substrate temperature to minimize intermixing followed by moderate annealing to improve the structural order. The Fe was deposited by means of electron beam evaporation at a rate of typically 0.5 layer per minute. The base pressure was always below 2×10^{-10} mbar. During evaporation, pressure raised to $<4\times10^{-9}$ mbar. Film deposition was done at a substrate temperature of 120 K, followed by a short ($\sim$1 minute) anneal to 300 K directly after the film deposition. This was done to increase the mobility of the atoms at the surface in order to improve the structure of the film.

The film thickness was determined using the signal-to-background ratio in the continuum region of the 2*p* x-ray absorption spectra recorded with linear light. This method, described in Ref. 25, relies on data from a library of ultrathin films which yield, to a very good accuracy, an exponential curve for the Fe signal-to-background ratio. This thickness determination method has been crosschecked with a wide variety of other calibration methods, e.g., Auger data, LEED, Curie temperatures, spin reorientation transitions, and quartz microbalance data. The fitting parameter derived from our data library is the electron yield sampling depth. We find an electron yield sampling depth value of 1.7 nm in the case of Fe thin films, Ref. 25. This exponential law for thickness determination, with the same value for the electron yield sampling depth, is also used by other workers based on independent data sets.[26] The estimated relative accuracy of this method is of the order of 0.2 ML for films thinner than 10 ML. The absolute accuracy is worse and can be expected to be of the order of 1 ML. However, the most accurate absolute thickness reference is the occurrence of the spin-reorientation transition.

III. RESULTS

Figure 1 shows Fe XMCD spectra recorded at 120 K for (a) 25 ML Fe on Ag(100) and (b) 3 ML Fe on Ag(100). For

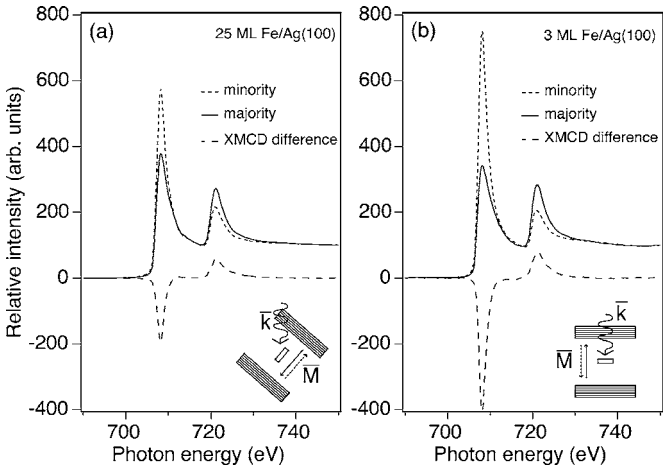

FIG. 1. XMCD spectra recorded at 120 K for a (a) 25 ML and (b) a 3 ML Fe film on Ag(100). The insets shows the experimental geometry.

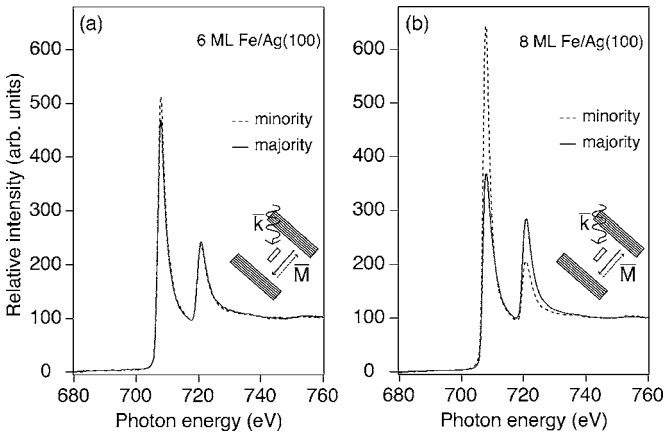

FIG. 2. XMCD spectra recorded at 120 K for (a), a 6 ML and (b), a 8 ML Fe film on Ag(100). In both cases a 45° x-ray incidence angle was used.

the data in Fig. 1(a) the angle of incidence was set to 45° to minimize saturation effects.[25] By investigating the angular dependence of the XMCD signal, the remanent magnetization was found to be in-plane as expected. For the 3 ML Fe film [see Fig. 1(b)], the incidence angle was set to 90° and the remanent magnetization was found out-of-plane. Analysis of the XMCD spectra by means of the magneto-optic sum rules gives values of the orbital and spin magnetic moment. These values are presented in Table I.

In Fig. 2 Fe XMCD spectra recorded at 120 K are shown for (a), 6 ML Fe on Ag(100) and (b), 8 ML Fe, respectively. For these Fe thicknesses no out-of-plane remanent magnetization was found. In Fig. 2(a) the magnetizing field was applied in-plane and the x-ray incidence angle was set to 30° grazing (60° relative to the surface normal). In this geometry we mainly measure the in-plane magnetization. In the case of the 6 ML Fe film, a very small magnetic contrast is visible, indicating that the in-plane magnetic remanence is very small. However, by adding two Fe layers to a total Fe thickness of 8 ML the film, as is evident in Fig. 2(b), exhibits a remanent magnetization very close to saturation. The values of the magnetic moments for these films are presented in Table I. The orbital moment, m_l, of the 3 ML film shows an increase of 125% compared to the 25 ML film. Only a small increase (of ~5%) of the spin moment, m_s, was observed. Large variations of the orbital moments, associated with changes in magnetic anisotropy causing a spin reorientation, has previously been reported by, e.g., Weller *et al.*[27] for Au/Co/Au structures.

At 6 ML, in the vicinity of the transition region from out-of-plane to in-plane magnetization, the remanent magnetization is very weak.[5] This significantly reduced moment is the result of domain formation at this critical reorientation thickness. This is confirmed by the M_l/M_s ratio which is essentially constant for films 6 ML and thicker. Adding two layers (a total of 8 ML) the Fe film exhibits an apparent saturated magnetization. The 8 ML Fe film shows an increase in m_l of 15% compared to m_l for the 25 ML Fe film, but no significant increase of in m_s.

We have performed *L*-edge EXAFS measurements on these films to probe the local crystallographic structure of the Fe atoms. Since the lattice mismatch between the Ag(100) surface and the Fe(100) film when rotated 45° is only 0.8%, Fe is expected to initially adopt the Ag(100) surface structure which would result in a bulklike bcc Fe growth.[15,28,29] However, our EXAFS measurements show that this is not the case. In Fig. 3(a) the *k*-weighted modulus of the Fourier transformed $\chi(k)$ is shown in real space for the 3 ML (dotted line) and the 25 ML (solid line) Fe films from Fig. 1. The EXAFS data were measured at 120 K using linearly polarized x rays at two incidence angles, 30°, and 90°, respectively. In Fig. 3(a) only the data recorded at 90° incidence angle are shown. In this geometry we mainly probe the local structure within the plane of the sample surface, whereas at 30° we mainly probe the structure perpendicular to the

TABLE I. Orbital (m_l) and spin (m_s) magnetic moments for 3, 6, 8, and 25 ML Fe on Ag(100). The 3 and 6 ML Fe film show out-of-plane magnetic moments, whereas the thicker films (3 and 6 ML Fe) show in-plane magnetic moments. The reduced moment for the 6 ML film is the consequence of domain formation at this critical reorientation thickness.

Fe/Ag(100)	m_l (μ_B)	m_s (μ_B)	m_l/m_s	Easy direction
3 ML	0.45	2.35	0.19	out-of-plane
6 ML	0.04	0.37	0.10	in-plane
8 ML	0.23	2.28	0.10	in-plane
25 ML	0.20	2.25	0.09	in-plane

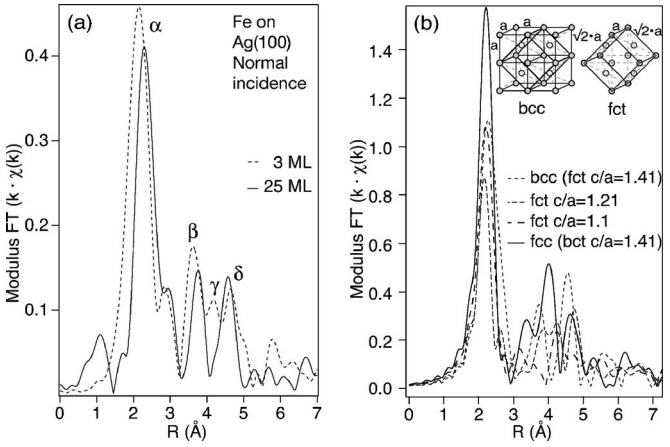

FIG. 3. (a) The k-weighted modulus of the Fourier transform $\chi(k)$ of the 3 ML and 25 ML Fe on Ag(100). The 25 ML film show the main feature at 2.30 Å and the characteristic double peak structure at 3.76 Å and 4.56 Å, which is a signature of bcc Fe Ref. (22). For the 3 ML Fe film the double peak features are now shifted to 3.63 Å and 4.64 Å, with an additional feature showing up at 4.17 Å. (b) EXAFS simulations using the FEFF 8.10 (Ref. 41) code show the k-weighted modulus of the Fourier transform for the bcc phase and various degrees of an extended bct (or fct) phase.

sample surface. From the spectra we see that the 25 ML film has its main peak at 2.30 Å and shows the characteristic double peak structure with sharp features at 3.76 Å and 4.56 Å, which is a signature of bcc Fe.[22,30,31] However, for the 3 ML Fe film the interpretation of the EXAFS result is not straightforward. The main peak is shifted 0.15 Å to 2.15 Å, with the double peak features shifted to 3.63 Å and 4.64 Å. In addition to these features, a new peak is found at 4.17 Å. This new feature should not be present in a bcc phase. The results are summarized in Table II.

In Fig. 3(b) EXAFS simulations are shown. The left-hand inset shows the lattice of the bcc cell with sides (a,a,a), which can also be viewed as a fct structure (right-hand inset) with the sides $(\sqrt{2}a,\sqrt{2}a,a)$. In the simulation the Fe cell has been expanded from the pure bcc phase, to the fcc phase in three steps. This expansion was done in such a way that the nearest neighbor distance was kept constant, resulting in a fcc cell with side $a=3.52$ Å $\left(a^{\mathrm{fcc}}=\sqrt{\frac{3}{2}}a^{\mathrm{bcc}}\right)$. The temperature in the simulations was set to 120 K (as in the experiment) with a Debye temperature of 477 K (as for bulk Fe). No anharmonic contributions to the potentials were included.

The pure bcc simulation agrees well with what was found for the 25 ML Fe film in Fig. 3(a), and what has been reported for bcc Fe L-edge EXAFS by Lemke *et al.*,[22] with peaks at 2.27 Å, 3.74 Å, and 4.56 Å. The experimental result of the structure of the 3 ML Fe film does not match the simulations for the bcc→fcc transition. However, the feature at 4.18 Å from Fig. 3(a) appears in the fcc simulation (here at ~4.02 Å) which suggests a mixed phase for the 3 ML Fe case, as discussed by Biedermann *et al.*[32,33] for the Fe/Cu(100) system. Furthermore, in the fcc simulation the main peak is found at 2.21 Å as compared to 2.15 Å and a feature at 4.61 Å that is experimentally found at 4.64 Å. However, the experimental peak at 3.62 Å does not agree so well with the simulated result at 3.37 Å. A simulation of a fcc structure with $a=3.62$ Å, i.e., assuming a constant atomic Fe volume, is presented in Table II. In this latter simulation we again fail to achieve good agreement with our experimental data.

In Fig. 4, a site dependent simulation for 3 ML Fe on Ag(100) is presented. The different sites A, B, and C, illus-

TABLE II. Peak positions for the most pronounced features obtained from EXAFS measurements of the 3, 6, 8, and 25 ML Fe films on Ag(100) for the 30° and 90° x-ray incidence angles. The peak positions α, β, γ, and δ are defined in Fig. 3(a). In addition, simulations using the FEFF 8.10 code are shown.

Fe on Ag(100) t	Angle	Peak positions (Å) α	β	γ	δ
3 ML	30°	2.15	3.66	4.18	4.64
	90°	2.15	3.63	4.17	4.64
6 ML	30°	2.21	3.68		4.67
	90°	2.23	3.69		4.66
8 ML	30°	2.21	3.69		4.70
	90°	2.25	3.68		4.66
25 ML	30°	2.30	3.76		4.56
	90°	2.30	3.76		4.56
Bulk bcc[a]		2.27	3.74		4.56
Bulk fcc[b]		2.21	3.37	4.02	4.61
Bulk fcc[c]		2.27	3.47	4.14	4.75

[a]Calculated for bcc Fe with $a=2.87$ Å.
[b]Calculated for fcc Fe with $a=3.52$ Å.
[c]Calculated for fcc Fe with $a=3.62$ Å.

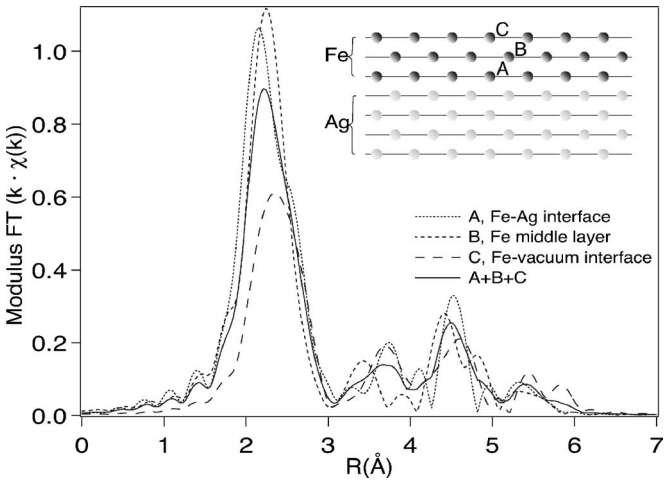

FIG. 4. Site dependent EXAFS simulations 3 ML Fe/Ag(100).

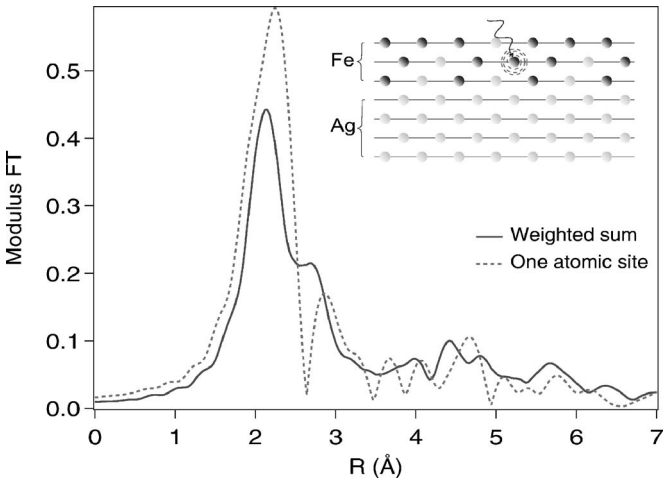

FIG. 5. EXAFS simulations of 3 ML Fe/Ag(100) including interface intermixing. The solid line represents the sum of all scattering paths from unique Fe sites in the model cluster. The agreement with experimental data is improved by including intermixing, although important differences still remains. The dashed line represents scattering from one particular site in the model cluster, where all scattering events include scattering from one or more Ag nearest neighbors. This curve contain structures found in the experimental EXAFS spectrum, but their overall intensity in the sum is too low as compared to experiment.

trated in the inset in Fig. 4, represent the Fe/Ag interface, the second Fe layer, and the Fe/vacuum interface, respectively. Here we have assumed a pure bcc structure for the Fe layers, initially occupying the fourfold hollow sites of the Ag surface, as described by Canepa *et al.*[15] The vertical spacing between the Fe layers was set to 2.87 Å (bulk value for Fe). For site *A*, representing the Fe/Ag interface, the main peak is found at 2.15 Å (instead of at 2.27 Å for bulk bcc), and we also find peaks at 3.74 Å, 4.11 Å, and 4.54 Å. At site *B*, representing the middle layer, the main peak is found at 2.24 Å and is stronger because of the higher coordination number. Additional peaks are found at 3.43 Å, which we attribute to the nearest Ag neighbors, and at 4.42 Å. The top-most site, *C*, representing the Fe/vacuum interface, exhibits a suppressed main peak due to the lower coordination number. Here the main peak is found at 2.36 Å, which is shifted 0.21 Å and 0.12 Å to larger distances compared to what was found for the interface and the middle layer, respectively. Moreover, here the double peaks are found at 3.71 Å and 4.63 Å. The solid line represents a weighted sum of the three individual layers, and the three main features are found at 2.21 Å, 3.68 Å, and 4.50 Å, respectively. The results of the simulation are summarized in Table III.

Even though these simulations show better agreement with the experimental data, the result is unsatisfactory. Motivated by earlier work,[15] we performed simulations to mimic various degree of interface intermixing. The geometries for the model clusters were obtained from *ab initio* density functional calculations using plane wave projector augmented wave method.[34,35] Geometry optimizations were carried out using accurate Hellman-Feynman forces in the generalized gradient approximation. Our calculations also provide layer-resolved spin moments for Fe atoms in the different environments in each layer. Interestingly, we find enhancement of the Fe spin moments which are largest at the interface ($2.7\mu_B$) and surface ($2.8\mu_B$) layers, the intermediate layer having a moment of $2.4\mu_B$. Thus, the average magnetic moment in the three-layer intermixed structure is $2.6\mu_B$.

In Fig. 5, Fe has been intermixed with Ag with the following concentrations: 50%, 25%, and 12.5% for the interface, middle, and top layer, respectively. The film structure is modeled as a relaxed bcc structure obtained from the calculations described above. The solid curve represents the weighted sum from all unique Fe sites in the cluster model, whereas the dashed curve is the EXAFS signal arising from

TABLE III. The positions of the most pronounced features from the *L*-edge EXAFS simulations from Fig. 4. The simulations were performed with the temperature and the Debye temperature set to 120 K and 477 K, respectively.

	Peak positions (Å)			
Fe on Ag(100) Site	α	β	γ	δ
A	2.15	3.74	4.11	4.54
B	2.24	3.43		4.42
C	2.36	3.71		4.63
Weighted sum	2.21	3.68		4.50

an Fe atom in the center of the film. It is clear that the simulation in Fig. 5 does not reproduce the experimental EXAFS for the 3 ML Fe film from Fig. 3. However, the dashed curve exhibits the spectral features we observe in the experimental EXAFS data. In particular, the feature around 4.1 Å (denoted γ) is only present when backscattering from one or more Ag atoms is considered. This finding supports the proposed model by Canepa *et al.*,[15] where the authors claim that Fe-Ag intermixing occur during deposition.

IV. DISCUSSION

Enhanced magnetic moments for the Fe/Ag(100) system as the film thickness is lowered has been reported both experimentally[9] and theoretically.[2,3,10–12] The values reported in the above-mentioned works agree fairly well with what is found in the present work. Sommers *et al.*[3] calculated a mean value of the magnetic moment of $3.05\mu_B$ for a 3 ML Fe film on Ag(100), whereas, e.g., Izquierdo *et al.*[2] reported a mean magnetic moment for the three topmost layers of $2.66\mu_B$. This is to be compared with our XMCD result for the 3 ML film, $m_{\mathrm{tot}}=2.80\mu_B$.

The magnetic properties of ultrathin Fe films are different on the Ag(100) substrate compared to, e.g., the similar Cu(100) substrate. The two systems both exhibit a SRT from in-plane to out-of-plane magnetization as the film thickness is lowered. However, the SRT is reported to occur at a lower Fe thickness in the case of Fe on Cu(100).[4] Also differences in the m_l and m_s are obvious when reducing the Fe film thickness. Hunter Dunn *et al.* report for 3.4 ML Fe on Cu(100), $m_l=0.23\mu_B$ and $m_s=3.33\mu_B$.[36] This is to be compared to our values for the 3 ML Fe on Ag(100) of $m_l=0.45$ and $m_s=2.35$ (bulk Fe values are $m_l=0.09$ and $m_s=2.25$). In the Fe/Cu(100) case, the high m_s has been explained by the existence of a "high spin" phase related to a suggested fct Fe structure on Cu(100). As Fe on Ag(100) is believed to initially grow bcc, the m_s could be expected to be lower. However, using scanning tunneling microscopy (STM) Biedermann *et al.*[32,33] suggested that Fe also initially adopts a bcc phase on Cu(100). The question then arises, why are the spin moments so different in the two cases?

In the experimental EXAFS results for the 3 and 25 ML Fe film in Fig. 3(a), we can identify the four main structures: α, β, γ, and δ, where the γ feature is only present for the 3 ML film. Comparing the experimental EXAFS results with the simulations in Fig. 3(b), we conclude that films thicker than 6 ML adopt the bcc structure. Some smaller shifts are observed in the main spectral feature α compared to the simulations using a pure bcc structure (see Table II). By studying the incidence angle dependence we observe a shift of 0.02 Å and 0.04 Å to higher values of the α peak at the 90° geometry for the 6 ML and 8 ML film, respectively. This indicates a larger lattice distance in-plane than out-of-plane.

The EXAFS results for the 3 ML Fe film deviate strongly from what is found for the thicker films. To model the structure of the 3 ML film, we attempted simulations where in which we expanded the bcc phase into the fcc phase while keeping the nearest neighbor distance constant. The simulation adopting the bcc bulk Fe does not reproduce the γ spectral feature. When expanding the bcc structure towards the fcc structure, we can follow the gradual change in the spectral features. In particular, the fcc simulation shows a peak near the position where we observe the γ feature in the experimental data. However, the fcc simulation does not reproduce the β peak. We conclude that the approach outlined above cannot reproduce the experimental EXAFS for the 3 ML Fe. Another attempt made with the fcc structure was to keep the Fe bulk atomic volume constant, requiring a lattice constant of $a^{\mathrm{fcc}}=3.62$ Å. This would result in a lattice mismatch of 12%, and the results of this latter simulation were far from what was found experimentally.

The site dependent EXAFS simulations in Fig. 4 show the importance of the Ag substrate. Here we can demonstrate large differences in the EXAFS signal when comparing the EXAFS simulation from the Fe surface layer (site *C*) and the Fe/Ag interface layer (site *A*). Interestingly the γ spectral feature, experimentally observed for the 3 ML Fe film from Fig. 3(a), is observed at site *A*. However, the weighted sum of the three-layer EXAFS simulations does not reproduce the EXAFS data for the 3 ML Fe film.

The reason why the 3 ML Fe film cannot adequately be modeled might be due to imperfections in the Fe layer growth. Canepa *et al.*[15] reported that island formation starts already within second Fe layer on Ag(100), with islands dimensions ~15–20 Å, and thus cannot be simulated as layers. Furthermore, the authors suggest that although precautions are taken, Fe-Ag intermixing occurs during deposition.

Our simulations of the EXAFS data using model clusters designed to mimic intermixing provide somewhat better agreement with experimental data. One could also consider scenarios where Ag segregates to the surface. However, with the growth conditions used in this study, i.e., sample kept at 120 K apart from a rapid anneal to room temperature, this is a minor effect.[37] In addition, a detailed path analysis reveals that multiple scattering including one or more Ag neighbors gives rise to structures in the EXAFS spectrum that correspond well to what we observe experimentally, which we have failed to model in any other way. This finding lends support to the proposition by Canepa *et al.*[15] The fact that these structures are not clearly visible in the average (confirm Fig. 5) indicates that our simulations underestimate the number of Fe sites where Ag atoms are nearest or next nearest neighbors. It is therefore reasonable to suggest that intermixing occurs to an even larger extent than what is proposed in Ref. 15. Such intermixing between film and substrate leads to a lower coordination for the Fe (reduced overlap between adjacent sites), and could then also explain the enhancement of the orbital moment for the 3 ML Fe film. However, intermixing at levels necessary to reproduce the experimental EXAFS spectrum should also have consequences for the magnetic properties of the samples. Effects of reduced dimensionality and exchange interaction would lead to a lowering of the critical temperature of the system. The critical temperature has not been measured for our samples. While Qiu *et al.*[38,39] report critical temperatures well above room temperature. These results would indicate that our measured values for the spin and orbital moments correspond to saturation values. However, our theoretical calculations suggest spin moments up to $2.8\mu_B$ for the intermixed

situation. The required scaling to reach saturation values as predicted by our calculations would result in a orbital moment, m_l, of $0.52\mu_B$/Fe atom. Even larger orbital moments have indeed been predicted theoretically for Fe impurities in a Ag matrix.[40]

V. CONCLUSIONS

By performing XMCD on Fe/Ag(100) we observed a reorientation of the magnetization as function of Fe thickness. For the measurements presented here (performed at 120 K) this transition occurs at 5–7 ML Fe. This reorientation is accompanied by an increase of the orbital moment for the out-of-plane phase of 125%. Only a minor increase of 5% in the spin moment is found. The *L*-edge EXAFS studies show that the thicker Fe films indeed grow in a bulklike bcc structure. Already at a thickness of 6 ML the bcc structure is clearly visible from our *L*-edge EXAFS experiment. For the thin films with out-of-plane magnetization, the local crystallographic structure is more complex and it is difficult to make a definitive assignment based on our present *L*-edge EXAFS data. While our modeling fails to perfectly reproduce the data, certain conclusions can be drawn from the various models presented. Simulations using different models based on sharp layers give only moderate agreement with our experimental data. We conclude that a degree of intermixing is present for the very thin films and improves the agreement when included in the modelling of the EXAFS data. It is also evident that varying degrees of tetragonal distortion are important to describe the structure of films in the ultrathin limit. In addition, we have identified scattering from Ag atoms as nearest or next nearest neighbors as important contributions in order to model all structures in the experimental EXAFS spectrum of the 3 ML film. Our findings suggest that even higher intermixing is required to explain our data. In a situation like this a large number of Fe sites will experience a reduced overlap where Ag atoms constitute nearest neighbors. This would influence the magnetic properties, and we propose that the effects of intermixing are responsible for the large orbital moment found for the 3 ML Fe film.

ACKNOWLEDGMENTS

This work was supported by the Swedish Research Council (Vetenskapsrådet) and the Göran Gustafsson Foundation.

[1] J. Langer, J. Hunter Dunn, A. Hahlin, O. Karis, R. Sellmann, D. Arvanitis, and H. Maletta, Phys. Rev. B **66**, 172401 (2002).
[2] J. Izquierdo, A. Vega, L. C. Balbas, D. Sanchez-Portal, J. Junquera, E. Artacho, J. M. Soler, and P. Ordejon, Phys. Rev. B **61**, 13639 (2000).
[3] C. Sommers, J. Zabloudil, C. Uiberacker, P. Weinberger, and L. Szunyogh, Phys. Rev. B **58**, 5539 (1998).
[4] D. P. Pappas, C. R. Brundle, and H. Hopster, Phys. Rev. B **45**, 8169 (1992).
[5] Z. Q. Qiu, J. Pearson, and S. D. Bader, Phys. Rev. Lett. **70**, 1006 (1993).
[6] J. G. Gay and R. Richter, Phys. Rev. Lett. **56**, 2728 (1986).
[7] N. C. Koon, B. T. Jonker, F. A. Volkening, J. J. Krebs, and G. A. Prinz, Phys. Rev. Lett. **59**, 2463 (1987).
[8] B. Heinrich, K. B. Urquhart, A. S. Arrott, J. F. Cochran, K. Myrtle, and S. T. Purcell, Phys. Rev. Lett. **59**, 1756 (1987).
[9] C. L. Wooten, J. Chen, G. A. Mulhollan, J. L. Erskine, and J. Markert, Phys. Rev. B **49**, 10023 (1994).
[10] H. Li, Y. S. Li, J. S. Quinn, D. Tian, J. Sokolov, F. Jona, and P. M. Marcus, Phys. Rev. B **42**, 9195 (1990).
[11] Z. Yumei, Z. Wenqing, Z. Lieping, and W. Dingsheng, J. Magn. Magn. Mater. **145**, L273 (1995).
[12] L. Szunyogh, B. Ujfalussy, and P. Weinberger, Phys. Rev. B **55**, 14392 (1997).
[13] B. Lazarovits, L. Szunyogh, and P. Weinberger, Phys. Rev. B **65**, 104441 (2002).
[14] A. Berger and H. Hopster, Phys. Rev. Lett. **76**, 519 (1996).
[15] M. Canepa, S. Terreni, P. Cantini, A. Campora, and L. Mattera, Phys. Rev. B **56**, 4233 (1997).
[16] H. Li and B. P. Tonner, Phys. Rev. B **40**, 10241 (1989).
[17] Jacob I. Egelhoff, W. F., and I. Jacob, Phys. Rev. Lett. **62**, 921 (1989).
[18] F. Ciccacci and S. De Rossi, Phys. Rev. B **51**, 11538 (1995).
[19] A. Hahlin, C. Andersson, O. Karis, J. Hunter-Dunn, and D. Arvanitis, Surf. Sci. **226-230**, 1675 (2003).
[20] B. T. Thole, P. Carra, F. Sette, and G. van der Laan, Phys. Rev. Lett. **68**, 1943 (1992).
[21] P. Carra, B. T. Thole, M. Altarelli, and X. Wang, Phys. Rev. Lett. **70**, 694 (1993).
[22] L. Lemke *et al.*, J. Phys.: Condens. Matter **10**, 1917 (1998).
[23] H. Jaffres *et al.*, Phys. Rev. B **61**, 14628 (2000).
[24] J. Hunter Dunn, A. Hahlin, O. Karis, D. Arvanitis, G. LeBlanc, A. Andersson, and L.-J. Lindgren, Synchrotron Radiation Instrumentation: Eighth International Conference on Synchrotron Radiation Instrumentation 705, 65 (2004), URL http://link.aip.org/link/?APC/705/65/1.
[25] D. Arvanitis, M. Tischer, J. Hunter Dunn, F. May, N. Mårtensson, and K. Baberschke, in *Spin Orbit Influenced Spectroscopies*, edited by H. Ebert and G. Schütz (Springer-Verlag, Berlin, 1996), and references therein.
[26] R. Nakajima, J. Stohr, and Y. Idzerda, Phys. Rev. B **59**, 6421 (1999); http://dx.doi.org/10.1103/PhysRevB.59.6421
[27] D. Weller, J. Stöhr, R. Nakajima, A. Carl, M. G. Samant, C. Chappert, R. Megy, P. Beauvillain, P. Veillet, and G. A. Held, Phys. Rev. Lett. **75**, 3752 (1995).
[28] D. Li, M. Freitag, J. Pearson, Z. Q. Qiu, and S. D. Bader, Phys. Rev. Lett. **72**, 3112 (1994).
[29] B. Jonker and G. Prinz, Surf. Sci. **172**, L568 (1986).
[30] Primarily due to what is referred to as the phase shift term in the EXAFS equation, the peak positions do not generally correspond to interatomic distances in real space. For more details on EXAFS please see, e.g., Ref. 31.
[31] J. Rehr and R. Albers, Rev. Mod. Phys. **72**, 621 (2000); http://dx.doi.org/10.1103/RevModPhys.72.621

[32] A. Biedermann, M. Schmid, and P. Varga, Phys. Rev. Lett. **86**, 464 (2001a).
[33] A. Biedermann, R. Tscheliessnig, M. Schmid, and P. Varga, Phys. Rev. Lett. **87**, 086103 (2001).
[34] G. Kresse and J. Hafner, Phys. Rev. B **47**, 558 (1993); http://dx.doi.org/10.1103/PhysRevB.47.558
[35] G. Kresse and J. Furthmüller, Phys. Rev. B **54**, 11169 (1996); http://dx.doi.org/10.1103/PhysRevB.54.11169
[36] J. H. Dunn, D. Arvanitis, and N. Mårtensson, Phys. Rev. B **54**, R11157 (1996).
[37] E. Vescovo, O. Rader, J. Redinger, S. Blugel, and C. Carbone, Phys. Rev. B **51**, 12418 (1995); http://dx. doi.org/10.1103/PhysRevB.51.12418
[38] Z. Q. Qiu, J. Pearson, and S. D. Bader, Phys. Rev. B **49**, 8797 (1994).
[39] Z. Q. Qiu, J. Pearson, and S. D. Bader, Phys. Rev. Lett. **67**, 1646 (1991).
[40] S. Frota-Pessôa, Phys. Rev. B **69**, 104401 (2004); http://link.aps.org/abstract/PRB/v69/e104401
[41] A. L. Ankudinov, B. Ravel, J. J. Rehr, and S. D. Conradson, Phys. Rev. B **58**, 7565 (1998).